DSP-based PDL Estimation and Localization in Multi-Span Optical Link Using Least Squares-based Longitudinal Power Monitoring

Minami Takahashi
NTT Network Innovation Laboratories
NTT Corporation
1-1 Hikarinooka, Yokosuka
Kanagawa, Japan
minami.takahashi.xr@hco.ntt.co.jp

Takeo Sasai
NTT Network Innovation Laboratories
NTT Corporation
1-1 Hikarinooka, Yokosuka
Kanagawa, Japan
takeo.sasai.cp@hco.ntt.co.jp

Etsushi Yamazaki
NTT Network Innovation Laboratories
NTT Corporation
1-1 Hikarinooka, Yokosuka
Kanagawa, Japan
etsushi.yamazaki.wk@hco.ntt.co.jp

Yoshiaki Kisaka
NTT Network Innovation Laboratories
NTT Corporation
1-1 Hikarinooka, Yokosuka
Kanagawa, Japan
yoshiaki.kisaka.dc@hco.ntt.co.jp

***Abstract*—We propose a method to identify position and amount of PDL in multi-span link by extending DSP-based longitudinal power monitoring. The method is linear least squares and provides high PDL sensitivity of 0.1 dB.**

Keywords—Optical transmission system, Longitudinal power monitoring, Linear least-squares method, Polarization-dependent loss

I. Introduction

Coherent optical fiber networks consist of a variety of optical in-line components including optical fiber couplers, isolators, filters, wavelength selective switches (WSS), and erbium-doped fiber-amplifiers (EDFA) [1-3]. The loss or gain imbalance of these components depends on the polarization and is called polarization-dependent loss (PDL). According to [1], WSS, which is considered the main source of PDL, has a maximum PDL of 0.6 dB per port. PDL in polarization-multiplexed digital coherent systems limits the transmission capacity and distance [4–7] and is one of the major factors degrading signal quality.

The power imbalance at the component output depends on the incident state-of-polarization (SOP). Thus, the PDL appears as a stochastically varying loss and results in stochastic variations in the system performance. Hence, to ensure reliability over its operational lifetime and avoid system outages, it is necessary to design the network with a PDL margin assuming the worst case [5]. The accumulated margins of individual PDL components increase the ambiguity of the estimated signal quality, thus limiting the transmission rate. If distributed PDLs that occur randomly and simultaneously in a multi-span link can be accurately monitored, such worst-case designs can be avoided and the transmission rates maximized.

For these reasons, various monitoring techniques have been proposed to estimate the physical parameters of transmission links including PDL [8–11]. Among these, the transceiver-based longitudinal power profile estimation (PPE) [12–18] has attracted interest because it is capable of estimating signal power evolution over multiple spans at a single coherent receiver without additional dedicated measuring equipment. Localization of PDL was recently demonstrated using PPE [19, 20]. However, this demonstration utilized the correlation method, and as pointed out in [15], the correlation method cannot estimate the true power, and thus it is difficult to estimate the true value of the PDL without a hardware-based calibration [20]. Furthermore, the spatial resolution of the correlation method is limited, as proved in [15].

In this paper, we propose a linear least squares algorithm for longitudinal PPE that visualizes polarization-wise signal power profiles in a multi-span link at a coherent receiver. As a result, the proposed method can localize the excess PDL positions with high spatial resolution and even estimate their true values. Our numerical results show that the proposed method successfully localized a PDL as low as 0.1 dB with a spatial step size of 1 km in a dual-polarization transmission over a 3-span × 50-km link.

II. Method

A. Principle of polarization-wise power profile estimation

Our PDL estimation method is an extended version of the least squares-based PPE proposed in [16, 18] to estimate the polarization-wise power profile based on the Manakov equation. The optical signal $\boldsymbol{A}(z,t) = \left[A_x(z,t), A_y(z,t)\right]^{\mathrm{T}}$ at position z and time t can be expressed using the loss (amplification) coefficients for x and y signals $\alpha_x(z)$ and $\alpha_y(z)$, the group velocity dispersion β_2, and the nonlinear coefficient γ as follows:

$$\frac{\partial \boldsymbol{A}}{\partial z} = -\frac{1}{2}\begin{pmatrix}\alpha_x(z) & 0\\ 0 & \alpha_y(z)\end{pmatrix}\boldsymbol{A} + j\frac{\beta_2}{2}\frac{\partial^2}{\partial t^2}\boldsymbol{A} - j\gamma\|\boldsymbol{A}\|^2\boldsymbol{A}. \quad (1)$$

The PDL can then be embedded in the matrix in the first term. Here, by transforming variables

$$A_x(z,t) = E_x(z,t)\exp\left(-\frac{1}{2}\int_0^z \alpha_x(z')\,dz'\right),$$
$$A_y(z,t) = E_y(z,t)\exp\left(-\frac{1}{2}\int_0^z \alpha_y(z')\,dz'\right),$$

the loss and nonlinear coefficients can be merged as

$$\frac{\partial \boldsymbol{E}}{\partial z} = j\frac{\beta_2}{2}\frac{\partial^2}{\partial t^2}\boldsymbol{E} - j\left(\gamma'_x(z)|E_x|^2 + \gamma'_y(z)|E_y|^2\right)\boldsymbol{E}, \quad (2)$$

$$\boldsymbol{\gamma}'(z) = \begin{pmatrix}\gamma'_x(z)\\ \gamma'_y(z)\end{pmatrix} = \frac{8}{9}\gamma\begin{pmatrix}P_x(z)\\ P_y(z)\end{pmatrix} = \frac{8}{9}\gamma P(0)\begin{pmatrix}\exp\left(-\int_0^z \alpha_x(z')dz'\right)\\ \exp\left(-\int_0^z \alpha_y(z')dz'\right)\end{pmatrix}. \quad (3)$$

Note that the power of $\boldsymbol{E}$ is normalized to 1. From (2), if $\gamma'_x(z), \gamma'_y(z)$ are obtained, the signal powers $P_x(z), P_y(z)$ can be estimated, assuming γ is constant. Therefore, our estimation target is $\boldsymbol{\gamma}'(z)$.

Fig. 1 shows the concept of the least squares-based estimation of $\boldsymbol{\gamma}'(z)$. In this work, the power profile $\boldsymbol{\gamma}'$ in (3) is estimated as the optimal $\boldsymbol{\gamma}'(z)$ of the digital twin link that minimizes the squared error between the received signal and the reference signal. In the digital twin-link, the transmission link, whose distance is L, is divided into K sections. The spatial step size of one section is Δz. The position is denoted by $z_k (k \in \{0, \cdots, K-1\})$, and thus $z_0 = 0$ and $z_{K-1} = L$. Let $\boldsymbol{E}[0] = \left[\boldsymbol{E_x}[0], \boldsymbol{E_y}[0]\right]^{\mathrm{T}}$ and $\boldsymbol{E}[L]$ be the transmitted and received signals with N samples, respectively. Also, $\boldsymbol{E}^{\mathrm{ref}}[L] = \left[\boldsymbol{E}_x^{\mathrm{ref}}[L], \boldsymbol{E}_y^{\mathrm{ref}}[L]\right]^{\mathrm{T}}$ is the reference signal obtained as an output of a digital twin simulating an optical link. In our method, the estimation of $\boldsymbol{\gamma}'(z)$ is formulated as the following least squares problem:

$$\begin{bmatrix}\widehat{\boldsymbol{\gamma}'_x}\\ \widehat{\boldsymbol{\gamma}'_y}\end{bmatrix} = \underset{\boldsymbol{\gamma}'_x, \boldsymbol{\gamma}'_y}{\operatorname{argmin}} I = \underset{\boldsymbol{\gamma}'_x, \boldsymbol{\gamma}'_y}{\operatorname{argmin}} \mathbb{E}\left[\left\|\boldsymbol{E}[L] - \boldsymbol{E}^{\mathrm{ref}}[\mathrm{L}]\right\|^2\right], \quad (4)$$

where $\boldsymbol{\gamma}'_{x/y}$ is a discretized version of $\gamma'_{x/y}(z)$.

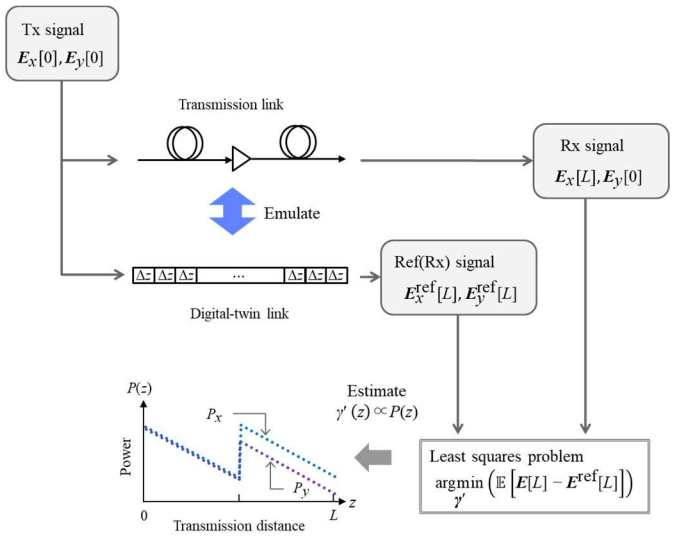

Fig. 1. Configuration of polarization-wise power profile estimation methods.

Subsequently, using the first-order perturbation method, $\boldsymbol{E}[L]$ and $\boldsymbol{E}^{\mathrm{ref}}[L]$ can be transformed into

$$I = \mathbb{E}\left[\left\|(\boldsymbol{E}_0 + \boldsymbol{E}_1) - \left(\boldsymbol{E}_0^{\mathrm{ref}} + \boldsymbol{E}_1^{\mathrm{ref}}\right)\right\|^2\right] = \mathbb{E}\left[\left\|\boldsymbol{E}_1 - \boldsymbol{E}_1^{\mathrm{ref}}\right\|^2\right], \quad (5)$$

where $\boldsymbol{E_0} = \left[\boldsymbol{E}_{0,x}, \boldsymbol{E}_{0,y}\right]^{\mathrm{T}}$ is a linear solution of (2) and $\boldsymbol{E}_1 = \left[\boldsymbol{E}_{1,x}, \boldsymbol{E}_{1,y}\right]^{\mathrm{T}}$ is a first-order perturbation solution. We used $\boldsymbol{E}_0 = \boldsymbol{E}_0^{\mathrm{ref}}$, assuming that the sampling rate for the linear terms satisfies the Nyquist theorem. The perturbation term $\boldsymbol{E}_1^{\mathrm{ref}}$ can be expressed as

$$\boldsymbol{E}_1^{\mathrm{ref}}[L] = \begin{pmatrix}\boldsymbol{E}_{1,x}^{\mathrm{ref}}\\ \boldsymbol{E}_{1,y}^{\mathrm{ref}}\end{pmatrix} = \boldsymbol{G}\begin{pmatrix}\boldsymbol{\gamma}'_x\\ \boldsymbol{\gamma}'_y\end{pmatrix} = \begin{pmatrix}\boldsymbol{G}_{xx} & \boldsymbol{G}_{xy}\\ \boldsymbol{G}_{yx} & \boldsymbol{G}_{yy}\end{pmatrix}\begin{pmatrix}\boldsymbol{\gamma}'_x\\ \boldsymbol{\gamma}'_y\end{pmatrix}, \quad (6)$$

where the k-th columns of $\boldsymbol{G}_i$ ($i \in \{xx, xy, yx, \text{and } yy\}$) are

$$(\boldsymbol{G}_{xx})_k = (-j\Delta z)\cdot \boldsymbol{D}_{L-z_k}\cdot\left(\left|\boldsymbol{E}_{0,x}[z_k]\right|^2 \boldsymbol{E}_{0,x}[z_k]\right),$$

$$(\boldsymbol{G}_{xy})_k = (-j\Delta z)\cdot \boldsymbol{D}_{L-z_k}\cdot\left(\left|\boldsymbol{E}_{0,y}[z_k]\right|^2 \boldsymbol{E}_{0,x}[z_k]\right),$$

$$(\boldsymbol{G}_{yx})_k = (-j\Delta z)\cdot \boldsymbol{D}_{L-z_k}\cdot\left(\left|\boldsymbol{E}_{0,x}[z_k]\right|^2 \boldsymbol{E}_{0,y}[z_k]\right),$$

$$(\boldsymbol{G}_{yy})_k = (-j\Delta z)\cdot \boldsymbol{D}_{L-z_k}\cdot\left(\left|\boldsymbol{E}_{0,y}[z_k]\right|^2 \boldsymbol{E}_{0,y}[z_k]\right).$$

$\boldsymbol{D}_{L-z_k}$ is the matrix that represents a CD operation corresponding to the distance of $L - z_k$. Each $\boldsymbol{G}_i$ refers to an N×K matrix.

Therefore, from (4), (5) and (6), the problem can be reduced to

$$\begin{bmatrix}\widehat{\boldsymbol{\gamma}'_x}\\ \widehat{\boldsymbol{\gamma}'_y}\end{bmatrix} = \underset{\boldsymbol{\gamma}'_x, \boldsymbol{\gamma}'_y}{\operatorname{argmin}} \mathbb{E}\left[\left|\begin{pmatrix}\boldsymbol{E}_{1,x}\\ \boldsymbol{E}_{1,y}\end{pmatrix} - \begin{pmatrix}\boldsymbol{G}_{xx} & \boldsymbol{G}_{xy}\\ \boldsymbol{G}_{yx} & \boldsymbol{G}_{yy}\end{pmatrix}\begin{pmatrix}\boldsymbol{\gamma}'_x\\ \boldsymbol{\gamma}'_y\end{pmatrix}\right|^2\right], \quad (7)$$

which can be solved by linear least squares. Since $\boldsymbol{\gamma}'_x$ and $\boldsymbol{\gamma}'_y$ are real vectors, the solution of (7) can be obtained as

$$\begin{bmatrix}\widehat{\boldsymbol{\gamma}'_x}\\ \widehat{\boldsymbol{\gamma}'_y}\end{bmatrix} = \left(\mathrm{Re}\left[\begin{pmatrix}\boldsymbol{G}_{xx} & \boldsymbol{G}_{xy}\\ \boldsymbol{G}_{yx} & \boldsymbol{G}_{yy}\end{pmatrix}^{\dagger}\begin{pmatrix}\boldsymbol{G}_{xx} & \boldsymbol{G}_{xy}\\ \boldsymbol{G}_{yx} & \boldsymbol{G}_{yy}\end{pmatrix}\right]\right)^{-1} \cdot \mathrm{Re}\left[\begin{pmatrix}\boldsymbol{G}_{xx} & \boldsymbol{G}_{xy}\\ \boldsymbol{G}_{yx} & \boldsymbol{G}_{yy}\end{pmatrix}^{\dagger}\begin{pmatrix}\boldsymbol{E}_{1,x}\\ \boldsymbol{E}_{1,y}\end{pmatrix}\right]. \quad (8)$$

Finally, the signal power profile for each polarization can be obtained using (3).

B. PDL estimation

Although the algorithm in the previous section can estimate the polarization-wise power profiles, it does not mean that the correct PDL can be estimated. This is because the power loss in each polarization depends on the incident SOP. Fig. 2 shows a conceptual diagram of a PDL medium with input optical signals at different SOPs. For simplicity, we assume here that the PDL medium has no birefringence.

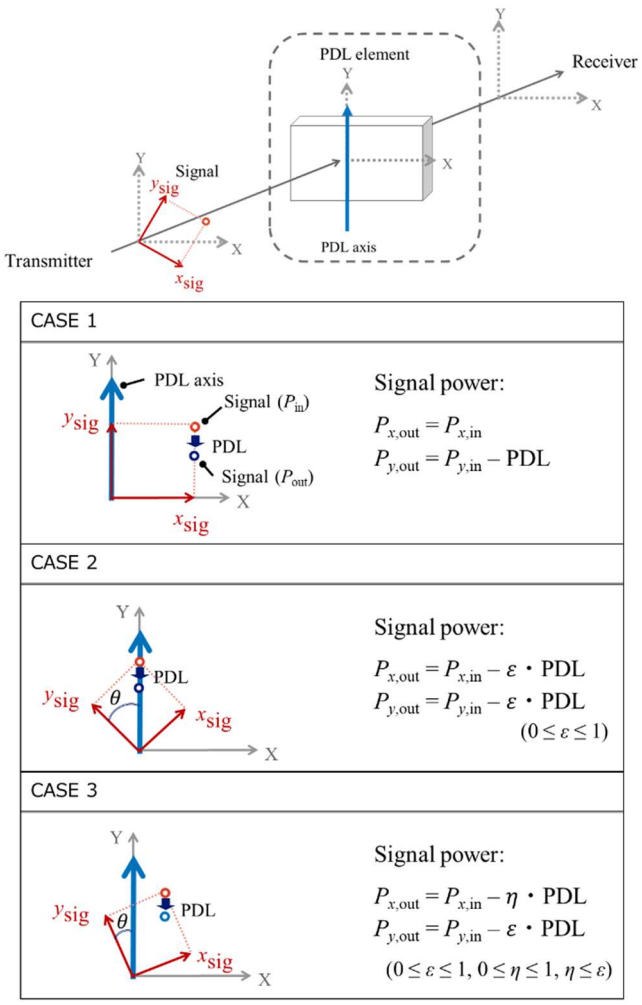

Fig. 2. Schematic diagram of a fiber span with PDL element showing the inclination (θ) between the PDL axis (blue) and signal axis (red) for several cases. Since the power loss in the x and y signal basis depends on θ, a signal basis should be aligned to the PDL axis for PPE to correctly estimate the PDL value.

To model the PDL, we use the Jones formulation to represent the electric field of the signal after it passes through the PDL element, as

$$\begin{pmatrix} E_{x,\text{out}} \\ E_{y,\text{out}} \end{pmatrix} = R(\theta)^{-1} F(\varphi)^{-1} \begin{pmatrix} 1 & 0 \\ 0 & \rho \end{pmatrix} F(\varphi) R(\theta) \begin{pmatrix} E_{x,\text{in}} \\ E_{y,\text{in}} \end{pmatrix}, \quad (9)$$

where

$$R(\theta) = \begin{pmatrix} \cos(\theta) & \sin(\theta) \\ -\sin(\theta) & \cos(\theta) \end{pmatrix} \text{ and } F(\varphi) = \begin{pmatrix} e^{j\frac{\varphi}{2}} & 0 \\ 0 & e^{-j\frac{\varphi}{2}} \end{pmatrix}.$$

In the above equation, $R(\theta)$ corresponds to the θ rotation of the polarization and $F(\varphi)$ is the retardance matrix. The power loss of both polarizations depends on θ and φ between the signal and PDL axes. For simplicity, only a single PDL element is assumed, and the loss is given as $\rho = 10^{\frac{-\text{PDL [dB]}}{20}}$ for one polarization only.

In the proposed method, it is necessary to align the coordinate system of the received and reference signals with that of the PDL to estimate the accurate PDL values. Therefore, by changing the polarization state, specifically, by sweeping (θ, φ) of the received signal and the reference signal, the polarization state that maximizes the power difference of two polarizations is obtained, and the PDL estimation is achieved.

III. Simulation Setup

A schematic representation of the simulation model and DSP algorithm is provided in Fig. 3. The transmitted signal was a single-channel 128-GBd dual-polarization probabilistic constellation-shaped (PCS) 64QAM signal (IR = 3.305, 21% FEC OH). The signal was Nyquist-shaped and had a root-raised-cosine filter with a roll-off factor of 0.1. The transmission link consisted of three 50-km spans. The input power was set to 5 dBm. Standard single-mode fiber (SSMF) was assumed, with a fiber loss of 0.2 [dB/km], a nonlinear coefficient γ of 1.3 [$W^{-1}km^{-1}$], and a group velocity dispersion β_2 of –21.7 [ps^2/km]. All EDFAs in the transmission link were set to constant gain mode and had a noise figure of 5 dB. PDL loading values of 0.1, 0.2, 0.3, 0.4, 0.5, and 1.0 dB were inserted at 75 km on the transmission link to emulate a PDL link. The SOP of the signal (θ and φ in (9)) at the input of the PDL element was randomly varied to verify our scheme can properly localize and estimate PDL for any SOP condition.

Fiber propagation was emulated by a split-step Fourier method with a spatial step size of 0.1 km and an oversampling ratio of 20 samples/symbol. After propagation, the signal was down-sampled to a ratio of 2 samples/symbol, and $E_1[L]$ was then calculated as $E_1[L] = E[L] - E_0[L]$. Polarization rotation was applied before PPE (8). The spatial step size was set to 1 km.

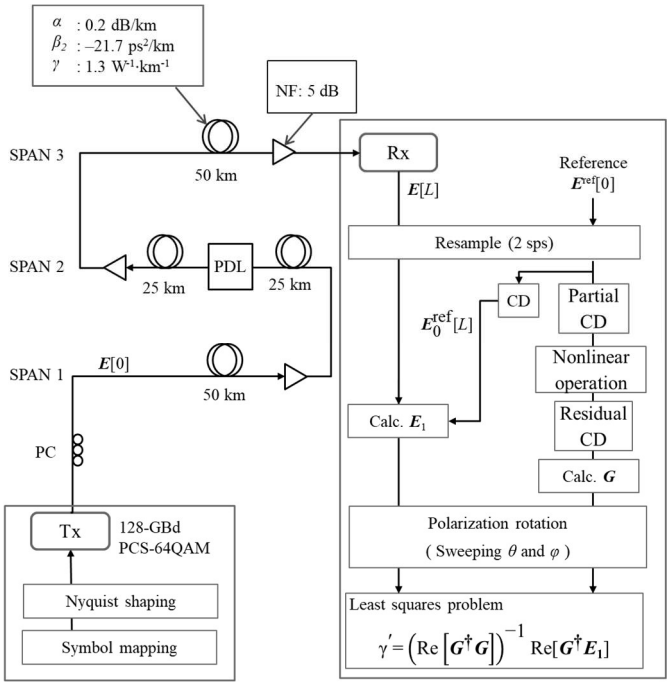

Fig. 3. Simulated optical transmission link model and proposed algorithm for polarization-wise PPE and PDL estimation.

IV. Simulation Results

A. Principle verification

First, we verified the effectiveness of the proposed method with a PDL value set to 2 dB. As explained in Section II.B, the SOPs of the received and reference signals should be aligned to the principal axis of PDL. Therefore, in Rx DSP, the SOP of the received and reference signals was changed to various SOPs to search for the correct PDL axis. Fig. 4 shows the power profiles of several polarization rotations (relative angles θ of 0, 15, 30, and 45 degrees). We can observe that the closer to the correct PDL axis ($\theta = 0$), the larger the power difference between polarizations. Here, the dependency on retardation φ is not shown since we confirmed through another simulation that sweeping φ in Rx DSP had negligible impact on the resulting power profiles, even though random φ values are applied at an emulated PDL in a link.

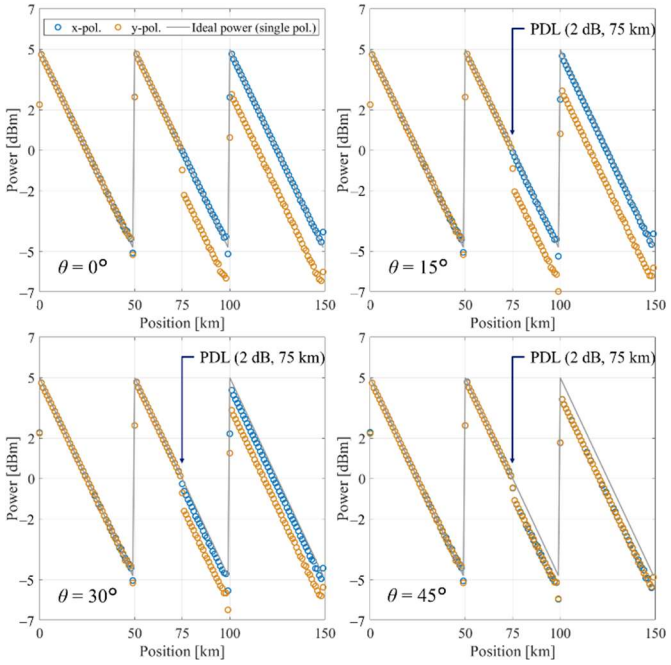

Fig.4. Estimated polarization-wise longitudinal power with various polarization rotation angles θ.

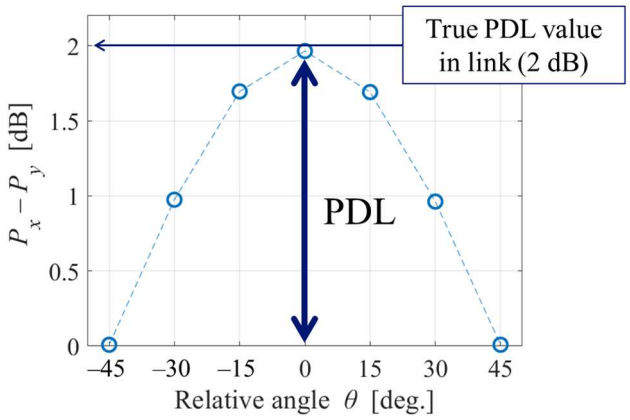

Fig.5. Power difference between polarizations with respect to relative angle between the PDL axis and signal axis. The power is shown for relative angles θ of 0, ±15, ±30, and ±45 degrees between the two axes. The signal power between each polarization was averaged over the 10 km after PDL loading.

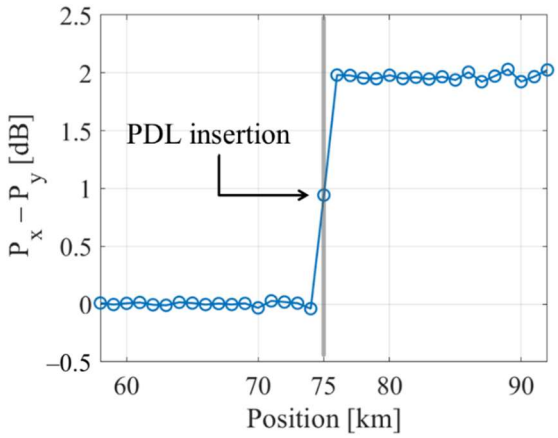

Fig.6. Power difference between polarizations in the vicinity of the PDL insertion point (with a relative angle $\theta = 0$).

The difference of estimated power between polarizations 10 km after the PDL location is shown in Fig. 5. The maximum power difference was obtained when $\theta = 0$ with a value of 1.96 dB, which is very close to the true PDL value set in a link, thus demonstrating the effectiveness of the proposed method. The power difference between each polarization in the vicinity of the PDL insertion point (at $\theta = 0$) is also shown in Fig. 6. Again, the spatial step size was set to 1 km. The variation of the power difference (PDL) was clearly observed at 75 km, which matches the actual PDL insertion point, thus indicating that the PDL was successfully localized with a spatial granularity of 1 km.

These results demonstrate that the proposed method can accurately estimate the value of the PDL and its position at Rx DSP even when the SOP of the signal changes in a link.

B. Estimation accuracy of PDL

Next, we evaluated the estimation accuracy of the PDL. The PDLs were set to 1 dB, 0.5 dB, 0.4 dB, 0.3 dB, 0.2 dB, and 0.1 dB. The results of PPE at each polarization for three spans are shown in Fig. 7. The power difference between polarizations near the PDL insertion point (at 75 km) is also shown in Fig. 8. Note that we searched beforehand for the best SOP that maximized the power difference between polarizations, and only the best case ($\theta = 0$) is shown in these figures. Other conditions were the same as in the previous section. As we can see, when the PDL values decreased, the power differences also decreased. From Fig. 8, we can estimate PDL values by averaging the power difference over the 10 km after PDL location. The estimated PDL values as a function of inserted PDL values are shown in Fig. 9. The estimated PDLs were 0.982 dB, 0.490 dB, 0.391 dB, 0.293 dB, 0.194 dB, and 0.0951 dB when the set PDL loadings were 1 dB, 0.5 dB, 0.4 dB, 0.3 dB, 0.2 dB, and 0.1 dB, respectively. For all cases, the estimated PDL values had absolute errors smaller than 0.1 dB and standard deviations smaller than 0.02 dB.

As stated earlier, a single PDL level is typical around 0.1 to 0.6 dB. Though our simulation did not consider several impairments (e.g., transceiver imperfection and inter-channel nonlinearity), these results demonstrate that the proposed method effectively localizes and estimates the excessive PDLs in a link at its upper performance limit.

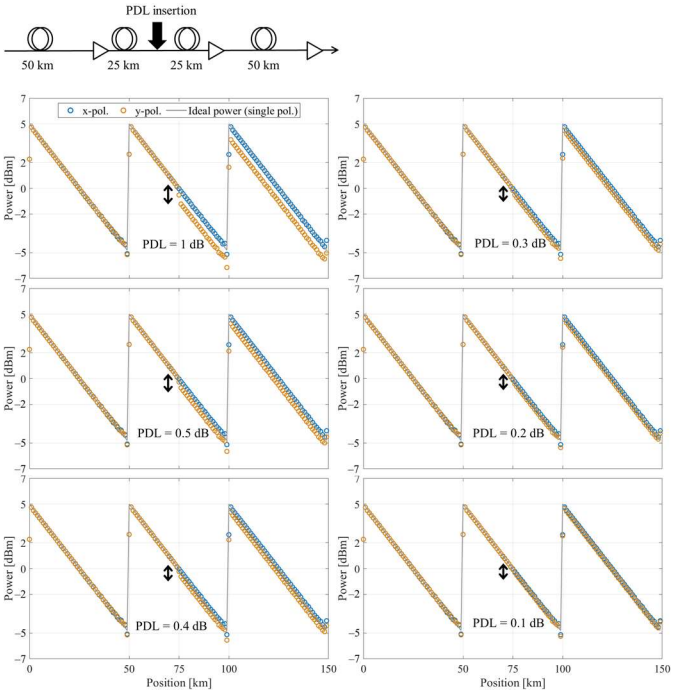

Fig.7. Estimated polarization-wise longitudinal power with various PDL levels. PDLs were set to 1 dB, 0.5 dB, 0.4 dB, 0.3 dB, 0.2 dB, and 0.1 dB.

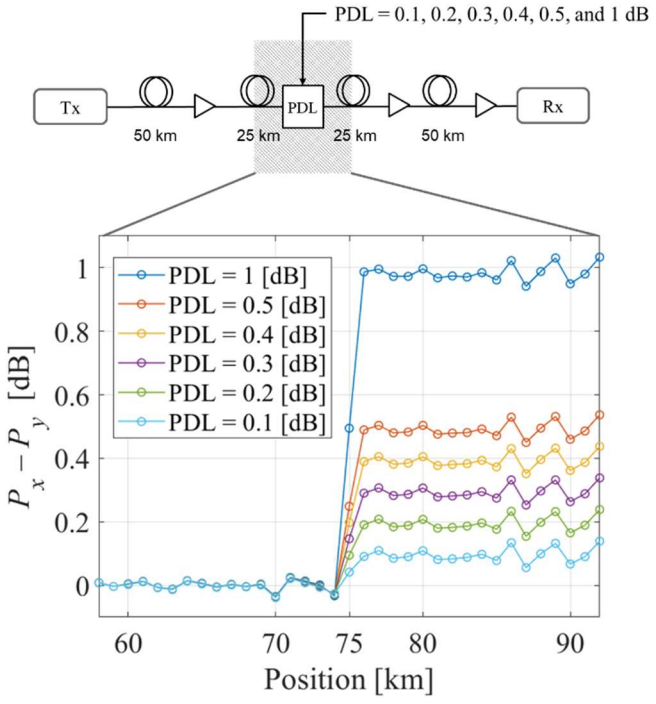

Fig.8. Power difference between polarizations in the vicinity of the PDL insertion point with various PDL levels.

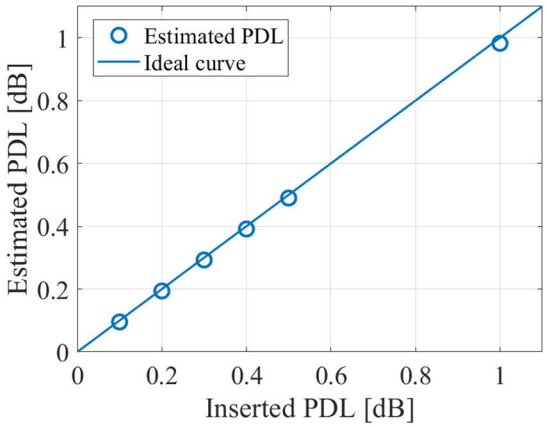

Fig.9. Estimated PDL as a function of inserted PDL.

V. Conclusion

In this paper, we proposed a linear least-squares algorithm for estimating polarization-wise longitudinal power profiles in Rx DSP, which enables the localization of excessive PDL in multi-span optical links and even the estimation of its value without any dedicated hardware devices. Our numerical results demonstrate that inserted PDLs ranging from 0.1 to 2 dB can be successfully localized and estimated with an absolute error < 0.1 dB.

References

[1] A. Dumenil, E. Awwad, and C. Méasson, "PDL in Optical Links: A Model Analysis and a Demonstration of a PDL-Resilient Modulation," in Journal of Lightwave Technology, vol. 38, no. 18, pp. 5017–5025, 15 Sept. 2020.

[2] A. El Amari, N. Gisin, B. Perny, H. Zbinden, and C. W. Zimmer, "Statistical prediction and experimental verification of concatenations of fiber optic components with polarization dependent loss," in Journal of Lightwave Technology, vol. 16, no. 3, pp. 332–339, March 1998.

[3] L. E. Nelson, M. Birk, P. Magill, A. Schex, and L. Rapp, "Measurements of the polarization dependent loss of multiple WDM channels in an installed, long-haul terrestrial link," IEEE Photonics Society Summer Topicals 2010, Playa del Carmen, Mexico, 2010, pp. 18–19.

[4] H. -M. Chin et al., "Probabilistic Design of Optical Transmission Systems," in Journal of Lightwave Technology, vol. 35, no. 4, pp. 931–940.

[5] M. Shtaif, "Performance degradation in coherent polarization multiplexed systems as a result of polarization dependent loss," Opt. Express 16, 13918–13932 (2008).

[6] L. E. Nelson et al., "Statistics of polarization dependent loss in an installed long-haul WDM system," Opt. Express 19, 6790–6796 (2011).

[7] L. S. Yan, Q. Yu, and A. E. Willner, "Demonstration of in-line monitoring and compensation of polarization-dependent loss for multiple channels," in IEEE Photonics Technology Letters, vol. 14, no. 6, pp. 864–866, June 2002.

[8] Y. Pointurier, "Design of Low-Margin Optical Networks," J. Opt. Commun. Netw. 9, A9–A17 (2017).

[9] I. Kim, X. Wang, O. Vassilieva, P. Palacharla, and T. Ikeuchi, "Maximizing Optical Network Capacity through SNR-Availability Based Provisioning," 2019 Optical Fiber Communications Conference and Exhibition (OFC), San Diego, CA, USA, 2019, pp. 1–3.

[10] L. E. Nelson, M. Birk, P. Magill, A. Schex, and L. Rapp, "Measurements of the polarization dependent loss of multiple WDM channels in an installed, long-haul terrestrial link," IEEE Photonics

Society Summer Topicals 2010, Playa del Carmen, Mexico, 2010, pp. 18–19.

[11] I. Sartzetakis, K. K. Christodoulopoulos, and E. M. Varvarigos, "Accurate quality of transmission estimation with machine learning," in Journal of Optical Communications and Networking, vol. 11, no. 3, pp. 140–150, March 2019.

[12] T. Tanimura, S. Yoshida, K. Tajima, S. Oda, and T. Hoshida, "Concept and implementation study of advanced DSP-based fiber-longitudinal optical power profile monitoring toward optical network tomography," Journal of Optical Communications and Networking, vol. 13, no. 10, E132–E141, 2021.

[13] M. Bouda, S. Oda, O. Vassilieva, M. Miyabe, S. Yoshida, T. Katagiri, Yasuhiko Aoki, Takeshi Hoshida, and Tadashi Ikeuchi, "Accurate Prediction of Quality of Transmission Based on a Dynamically Configurable Optical Impairment Model," J. Opt. Commun. Netw. 10, A102–A109 (2018).

[14] Z. Tao, L. Dou, T. Hoshida, and J. C. Rasmussen, "A Fast Method to Simulate the PDL Impact on Dual-Polarization Coherent Systems," in IEEE Photonics Technology Letters, vol. 21, no. 24, pp. 1882–1884, 15 Dec. 2009.

[15] T. Sasai, E. Yamazaki, and Y. Kisaka, "Performance Limit of Fiber-Longitudinal Power Profile Estimation Methods," in Journal of Lightwave Technology, pp. 1-13, 2023.

[16] T. Sasai, E. Yamazaki, M. Nakamura, and Y. Kisaka, "Proposal of Linear Least Squares for Fiber-Nonlinearity-Based Longitudinal Power Monitoring in Multi-Span Link," 2022 27th OptoElectronics and Communications Conference (OECC) and 2022 International Conference on Photonics in Switching and Computing (PSC), Toyama, Japan, 2022, pp. 1–4.

[17] T. Sasai et al., "Digital Longitudinal Monitoring of Optical Fiber Communication Link," in Journal of Lightwave Technology, vol. 40, no. 8, pp. 2390–2408, 15 April 2022.

[18] T. Sasai, M. Nakamura, E. Yamazaki, H. Nishizawa, and Y. Kisaka, "0.77-dB Anomaly Loss Localization Based on DSP-Based Fiber-Longitudinal Power Estimation Using Linear Least Squares," 2023 Optical Fiber Communications Conference and Exhibition (OFC), San Diego, CA, USA, 2023, W1H.4.

[19] M. Eto, K. Tajima, S. Yoshida, S. Oda, and T. Hoshida, "Location-resolved PDL Monitoring with Rx-side Digital Signal Processing in Multi-span Optical Transmission System," 2022 Optical Fiber Communications Conference and Exhibition (OFC), San Diego, CA, USA, 2022, pp. 1–3.

[20] A. May, E. Awwad, P. Ramantanis, and P. Ciblat, "Receiver-Based Localization and Estimation of Polarization Dependent Loss," 2022 27th OptoElectronics and Communications Conference (OECC) and 2022 International Conference on Photonics in Switching and Computing (PSC), Toyama, Japan, 2022.